BioCore
Exploring Scientific Community

International Journal of Nanotechnology in Medicine & Engineering

Research Article
ISSN 2474-8811

Suppression of in Vitro Wound Healing Process in Monolayers of Lung Epithelial Cells by Poly-dispersed-acid-functionalized-single-walled Carbon Nanotubes and Its Mechanism.

Sushreesangita P. Behera[1],Rajiv K. Saxena[1]*

[1]Faculty of Life Sciences and Biotechnology South Asian University, New Delhi, India

Abstract

Repair mechanisms following lung injury involve proliferation and migration of healthy epithelial cells in the vicinity of the injury to the site of injury. We have used a model of in vitro wound repair using monolayers of LA4 and A549 epithelial cell lines to study changes in the expression of molecules involved in cell-to-cell adhesion and migration during wound healing process. We have demonstrated that the poly-dispersed acid-functionalized-single-walled carbon nanotubes (AF-SWCNTs) block cell migration and cell division in this model and correlated this inhibition with molecular changes. Flow cytometric and confocal microscopy studies indicated that AF-SWCNTs were efficiently internalized by both cell lines. Examination of the wound repair process by live-cell imaging time-lapse micrography indicated that the active cell proliferation around the scratch wound area was completely blocked by AF-SWCNTs in LA4 cells and significantly inhibited in A549 cells. Assessment of cell migration across permeable membrane in trans-well cultures further indicated a marked inhibition of migration of both cells by AF-SWCNTs. Cellular expressions of proteins like β-catenin, NM-myosin, and vimentin having crucial roles in cell migration were suppressed by AF-SWCNTs whereas the expression levels of E-cadherin and Claudin-1, involved in cell-cell adhesion remained unaltered. Sustained cell to cell adhesion in presence of AF-SWCNTs prevents cells to detach and migrate. Our results indicate that AF-SWCNT induced blockage of cell division and migration of epithelial cells and prevention of the detachment of cells from the monolayers needed for wound repair may be important factors responsible for suppression of wound repair process in monolayers of lung epithelial cells.

Keywords: Carbon Nanotubes; Cell Migration; Cell Adhesion; Lung Epithelial Cells; Flow Cytometry; Confocal Microscopy; Live Cell Imaging.

Corresponding author: **Rajiv K. Saxena**

Faculty of Life Sciences and Biotechnology,South Asian University, Akbar Bhawan, Chanakyapuri,New Delhi, India

E-mail: rajivksaxena@hotmail.com

Citation: Sushreesangita P. Behera and Rajiv K. Saxena (2020), Suppression of in Vitro Wound Healing Process in Monolayers of Lung Epithelial Cells by Poly-dispersed-acid-functionalized-single-walled Carbon Nanotubes and Its Mechanism. Int J Nano Med & Eng. 5:3.

Received: August 06, 2020
Accepted: August 21, 2020
Published: September 15, 2020

Introduction

Carbon nanotubes (CNTs) first reported by Iijima in 1991 [1], have exceptional mechanical, thermal, and electrical properties, and have found multiple commercial usage in industry as well as in biomedical fields [2-5]. The growing demand has led to an exponential increase in the production of CNTs which is about 15000 metric tons now growing at an annual rate of about 30% (nanowerk.com). Since there are no efficient mechanisms for the degradation of CNTs in nature, accumulation of CNTs in the environment and its adverse health effects are of widespread concern [6-9]. Pristine single-walled carbon nanotubes are highly hydrophobic and exist as large agglomerates insoluble in aqueous media. CNTs can however be converted to poly-dispersed hydrophilic form by the process of acid functionalization, which results in the attachment of carboxyl and sulfonate groups on carbon atoms in CNT walls [10-12]. The resulting acid-functionalized single-walled carbon nanotubes (AF-SWCNTs) are well dispersed in aqueous media and interact well with cells. Our group has been studying the interactions of AF-SWCNTs with cells in several biological systems, and have demonstrated modulatory effects of AF-SWCNTs on the activation and functioning of T cells [13-14], B cells [15], antigen presenting cells [16-18], hematopoietic activity in bone marrow [8, 19], and lung epithelial cells [11, 16-17]. In the present study, we have focused on the modulation of adhesion and migration of lung epithelial cells by AF-SWCNTs.Cell adhesion and migration seen from the perspective of lung physiology, are crucial to sustain the integrity

of lung alveoli and their repair after injury. Alveoli are lined by lung type I and II epithelial cells and cell-to-cell adhesion between the epithelial cells results in an epithelial cell lining through which gaseous exchange takes place. Alveolar surface is also under constant onslaught of airborne pathogens and pollutants that may often cause localized injury and disruption of the epithelial cell surface lining the alveoli. Efficient mechanisms are in place to ensure that following injuries the epithelial cell layers get repaired quickly to permit uninterrupted life-sustaining exchanges of oxygen and carbon dioxide [20-21]. It is believed that epithelial cells in the vicinity divide and migrate to the site of injury to fill the gap in epithelial cell layers [20, 22-24]. This repair response requires that the epithelial cells participating in the repair mechanism divide and migrate to the site of injury. Factors that alter the adhesion and migratory functions of epithelial cells may therefore influence the repair process. In the present study, we have focused on the modulation of cellular adhesion and migration of lung epithelial cells by carbon nanotubes using two cell lines (LA4 murine and A549 human lung epithelial cell lines) as models. Our results demonstrated that AF-SWCNTs are internalized in significant amounts by the epithelial cells. Furthermore, AF-SWCNTs significantly inhibited the cell migration process in both LA4 and A549 cells by interfering with the expression of crucial marker proteins involved in cell migration. These findings provide an insight into the mechanism of interference in cell migration and adhesion in lung epithelial cells by acid-functionalized carbon nanotubes and the molecules involved in this effect.

Materials and Methods

Cells and Reagents

LA4 (a murine lung epithelial cell line) and A549 (a human alveolar epithelial cell line) were obtained from American Type Cell Culture, cultured in a humidified incubator at 37°C and 5% CO_2 and maintained in RPMI 1640 culture medium supplemented with 2 mM glutamine, 4.5g glucose per litre, 10 mM HEPES buffer (pH 7.2), gentamycin (10 µg/ml), and fetal bovine serum (10% V/V).

Reagents and other supplies

Acid-functionalized single-walled carbon nanotubes prepared by the arc-discharge method and carboxylated by nitric acid and sulfuric acid treatment, were procured from Sigma-Aldrich (Cat No. 652490). The material was in the form of black powder that was >90% carbon and 5-8% metals with 1-3% carbon atoms as carboxyl acid groups. The average dimension of the nanotubes was 1.4 nm and its bundles ranged 4-5 nm in width and 500-1500 nm in length. The product was easily dispersible in water at the concentration used. Zetasizer analysis indicated a zeta potential of -45.3 mV and an average size of 178 dnm (Supplementary Figure 1A). TEM images of AF-SWCNTs indicated the fibrous structure (Supplementary Figure 1B). Mid and near-infrared spectroscopic results provided by Sigma-Aldrich are given in Supplementary Figure 1C.N-Hydroxysuccinimide (NHS), 1-ethyl-3-(3-dimethylaminopropyl) carbodiimide (EDAC), 2-(N-morpholino) ethane sulfonic acid (MES), and Transwell 24 well plates were procured from Sigma Aldrich, USA. Alexafluor 633 hydrazide was obtained from Molecular Probes (Carlsbad, CA, USA). RPMI 1640 culture medium supplemented with glutamine (2 mM), HEPES buffer pH 7.2 (10 mM), gentamycin (10 µg/ml), and fetal bovine serum (10% V/V) were purchased from Himedia, India. Centricon 3kDa centrifugal filter device was obtained from Millipore (Billerica, MA, USA). Monoclonal antibody against NM-myosin (ab55456) was procured from Abcam (Cambridge, UK). ß-catenin (MA110056), Vimentin (OMA1-06001), E-cadherin (PA5-16766), and Claudin-1 (PA516833) antibodies were purchased from Thermo Fisher (Waltham, USA). Live cell imaging dishes (35×10 mm) were purchased from Eppendorf (Hamburg, Germany).

Tagging of fluorochrome to AF-SWCNTs

Fluorescence tagged AF-SWCNTs (FAF-SWCNTs) were obtained by chemically tagging the fluorochrome Alexa Fluor 633 to AF-SWCNTs using MES buffer containing EDAC and NHS as described elsewhere [8], and were sonicated before use. The tagging efficiency of fluorophore to AF-SWCNTs was above 90% [14].

Flow Cytometry

For studies on the uptake of FAF-SWCNTs, LA4 and A549 cells were incubated in 24 well plate [0.2×106/ml/well] with or without 10 µg/ml of FAF-SWCNTs. The cells were harvested by trypsinization, washed with PBS, and analysed on a FACS Verse flow cytometer (BD Bioscience).

Confocal Microscopy

To study the uptake and localization of the FAF-SWCNTs, LA4 and A549 cells were cultured [0.05×106/ml/well] on a coverslip in a 12 well culture plate, incubated with 10 µg/ml of the FAF-SWCNTs for 24 hours, washed twice with PBS, and fixed with 4% paraformaldehyde. Nuclei were counterstained with Hoechst 33322 dye as described previously [15]. Coverslips were mounted onto the glass slide with 50% glycerol and slides were visualized on a Nikons A1R Confocal Laser Scanning Microscope.

Scratch Wound Assay and Live Cell Imaging for Video Recording

To study the in vitro wound repair process, LA4 and A549 cells were cultured at a cell density of [0.5×106 cells/ml/well], in a 6 well culture plate. After 24 hours, when complete monolayers were formed, AF-SWCNTs were added at concentrations of 0 (control), 20, 50 and 100 µg/ml for 6 hours. The monolayers were then scratched with the help of 200 µl pipette tip to create linear wounds. Monolayers were washed to remove dislodged cells and the culture medium replaced with AF-SWCNTs suspensions at original concentrations. The wounds were observed and photographed at 0, 12, 24 and 36 hours by NIS-Nikons phase contrast microscope. The residual wound areas were measured using the NIH Image J software. The assay was performed in triplicate and repeated thrice. For live cell imaging videography, a culture dish was placed on the live imaging stage of microscope comprising transparent culture chamber maintained at 37°C and with 5% CO_2 in air environment. Time-lapse differential interference contrast (DIC) images were acquired (1 per 10 minutes) for 36 hours.

Trans-well assay of Cell migration

To investigate the effect of the AF-SWCNTs on cell migration, trans-well culture system (24-well trans-well plates with 8-µm pore size polycarbonate filter between the top and bottom wells, Catalog no.3422, Corning, Life Science) was used. Cells at a density of [3.0×104/100µl/well] were cultured in the upper chambers of the trans-well unit in serum-free medium. The lower chambers of the trans-wells contained normal culture medium containing 10% FBS as chemoattractant. Cells in the upper chambers were untreated (controls) or treated with 50 and 100 µg/ml of AF-SWCNTs and incubation carried out at 37°C in a 5% CO_2 atmosphere for 24 hours. The residual cells on the upper side of the trans-well membrane were removed using a cotton swab and the membranes were fixed with 70% alcohol and stained with crystal violet to visualized the migrated cells below the membrane. The number of migrated cells was counted with the help of NIH Image J software.

Western Blotting

Western blot analysis was carried out as described previously [25] with slight modifications. Briefly, LA4 and A549 cells were cultured with or without 50 and 100 µg/ml of AF-SWCNTs for 48 hours. Cells were washed twice with ice-cold PBS and incubated in radio-immuno-precipitation assay (RIPA) lysis buffer containing a cocktail of protease

inhibitors at 4°C for 20 min. and then stored at -80° C overnight. After 24 hours cell lysates were collected, sonicated 3 times for 5 sec. each and analysed for protein content using the BCA protein assay kit (Thermo Fisher Scientific). Samples, 30 µl, (1 µg/µl of cell lysate proteins) per lane were resolved by SDS-PAGE (8% sodium dodecyl sulfate-polyacrylamide gel electrophoresis) along with pre-stained protein ladder and transferred onto PVDF membranes (Invitrogen). The transferred membranes were blocked for 1 hour using 5% BSA in TBST (25 mm Tris-HCl, pH 7.4, 125 mm NaCl, 0.05% Tween 20) and incubated with the appropriate primary antibodies (ß catenin, NM-myosin II, Vimentin, E-cadherin and Claudin-1) at 4°C overnight. Membranes were washed twice with TBST for 5 min. and incubated with horseradish peroxidase-coupled isotype-specific secondary antibodies for 1 h at room temperature. The immune complexes were detected by enhanced chemiluminescence detection system (Bio-Rad) and quantified using NIH Image J software.

Intracellular immunofluorescence Staining

LA4 and A549 cells were cultured to confluence on glass cover slips and treated with 100 µg/ml of AF-SWCNTs for 24 hours, fixed with 4% paraformaldehyde in PBS. The samples were washed two times, permeabilized with 0.1% Triton X-100 for 15 min. and blocked with 5% bovine serum albumin in PBST for 1 hour before staining with ß-catenin and NM-myosin (1:400 dilution) primary antibody, followed by Alexa Fluor 488-conjugated secondary antibody (Thermo Fisher). The nuclei were stained with Hoechst 33342 dye and coverslips were mounted with 50% glycerol for visualization using Nikons confocal laser scanning microscope.

Statistical Analysis

All experiments were repeated at least three times. Results are expressed as mean ±SEM. The paired t-test was performed to define the significance of all the experiments. Statistical analyses were performed using Sigma Plot software (Systat Software, San Jose, CA).

Results

Uptake of FAF-SWCNTs by LA4 and A549 cells

The aim of this study was to examine the effect of AF-SWCNTs on cell adhesion and migration in lung epithelial cell lines. Cell lines used were LA4 (a murine lung epithelial cell line) and A549 (a human lung epithelial cell line). Flow cytometry as well confocal microscopic studies indicated that both cells efficiently internalized FAF-SWCNTs. Consolidated results of flow cytometry given in Figure 1 (panel A) show the kinetics of uptake of FAF-SWCNTs by LA4 and A549 cells and indicate that at 12 and 24 h time points, almost all cells were positive for FAF-SWCNTs uptake. The Mean Fluorescence Intensity (MFI) data in the same figure (right Y axis) shows that the A549 cells take up relatively more FAF-SWCNTs than the LA4 cells. For confocal microscopy, cells exposed to FAF-SWCNTs were counterstained with Hoechst 33342 dye to visualize blue stained nuclei while FAF-SWCNTs could be visualized by its red fluorescence. Results in Figure 1B (top panel) show that the red fluorescence of FAF-SWCNTs was generally localized in the cytoplasmic area of the LA4 cells. Z-sectioning images (2, 2.5 and 3 µm depths) in Figure 1B (lower panel) show that the FAF-SWCNTs were localized in the cytoplasm with relatively poor uptake in nuclei. Similar data for A549 cells are presented in Figure 1C.

Inhibition of in vitro wound healing by AF-SWCNTs

It is well known that if a scratch is made in a monolayer of epithelial cells, cells in the surrounding area move to fill the wound area [26-28]. Effect of AF-SWCNTs was examined in this scratch assay of wound healing. Results in the top panel of Figure 2 show that in the case of monolayers of control LA4 and A549 cells, the scratch was completely filled by 36 hours post-scratch. However, addition of AF-SWCNTs resulted in a significant inhibition of gap-filling by both cells. Kinetics data of filling of the scratch for control and AF-SWCNTs treated LA4 and A549 cells are shown in the bottom panel of Figure 2. In control cells, the scratch gap was completely filled by 36 hours but in the presence of 20, 50 or 100 µg/ml of AF-SWCNTs, only 30 to 50% of the gap area could be filled in both cases. These results indicate that AF-SWCNTs significantly reduced the ability of cells to fill the scratch wound.

Live cell imaging to study the wound healing process

Scratch wound healing in LA4 and A549 cells was also recorded on a live cell imaging system. Video clips of cellular movement during the wound healing process are provided in the legends to Figure 3. There was a significant cell division activity around the scratch wound area that could be visually assessed by counting the number of dividing cells from the video clips of both control and AF-SWCNTs treated cells. Results in the left panels of Figure 3 show that within the time period of 36 hours, 215 of the total LA4 cells and 170 of the A549 cells in the view field divided in control plates and that number went down to about 60 each for both LA4 and A549 cells if 100 µg/ml of AF-SWCNTs were added to the culture medium. These results indicated that AF-SWCNTs suppressed the cell division activity around the scratch wound in both cell lines. Cell divisions in 5 hour time intervals during the wound-healing assay were also counted for control and AF-SWCNTs treated culture wells. Data in the right panels of Figure 3 show that for LA4 cells, the cell divisions in AF-SWCNTs treated cells continued till 10 hours and then fell sharply to zero at later time periods. For A549 cells however, the cell division activity continued in AF-SWCNTs treated cells albeit at a significantly lower level than that in the control cells. The total number of cells in the view field for control and AF-SWCNTs treated LA4 and A549 cells were very similar and the observed fall in cell division activity was not due to differences in the total number of cells in the view fields.

Migration of LA4 and A549 cells in trans-well assay system

Trans-well migration assay has been used by many investigators [29, 30] to study the cellular migration across a membrane with 8 µm pores separating the top and bottom culture wells.Results in Figure 4 (upper panels) show the migrated cells underneath the trans-well membrane, stained with crystal violet for control and AF-SWCNTs treated LA4 and A549 cells. These results show that a significantly lower number of cells migrated if AF-SWCNTs (50 or 100 µg/ml doses) were added to the culture. Data for the numbers of cells that migrated in control and AF-SWCNTs treated cultures are given in the lower panel of Figure 4. These results clearly show that there was dose dependent inhibition of cellular movement in cells exposed to AF-SWCNTs.

Modulation of the expression of molecules involves in cellular adhesion and migration by AF-SWCNTs

As a significant inhibitory effect of AF-SWCNTs was seen on the migration of LA4 and A549 cells in the wound healing and trans-well migration assays, we investigated the expression levels of some selected crucial proteins known to be involved in the regulation of cell migration and adhesion, namely ß-catenin, Non Muscle Myosin II (NM-myosin II), Vimentin, E-cadherin and Claudin-1. Western blotting results in Figure 5 show that ß-catenin was significantly downregulated in LA4 and A549 cells exposed to 100 µg/ml of AF-SWCNTs; the decline was 98% and 79% in LA4 and A549 respectively (quantitative band intensity in first from top panel). Expression of other crucial proteins like NM-myosin II and Vimentin were like-wise affected by AF-SWCNTs exposure. LA4 cells, treated with AF-SWCNTs (100 µg/ml), the expression of NM-myosin and Vimentin was 63% and 58% downregulated, whereas in A549 cells, the expression of NM-myosin and Vimentin was found to be 76% and 56% downregulated in comparison to the control cells. The expression of cell adhesion molecules like E-cadherin and Claudin-1 was not significantly altered in AF-SWCNTs treated LA4 and A549 cells

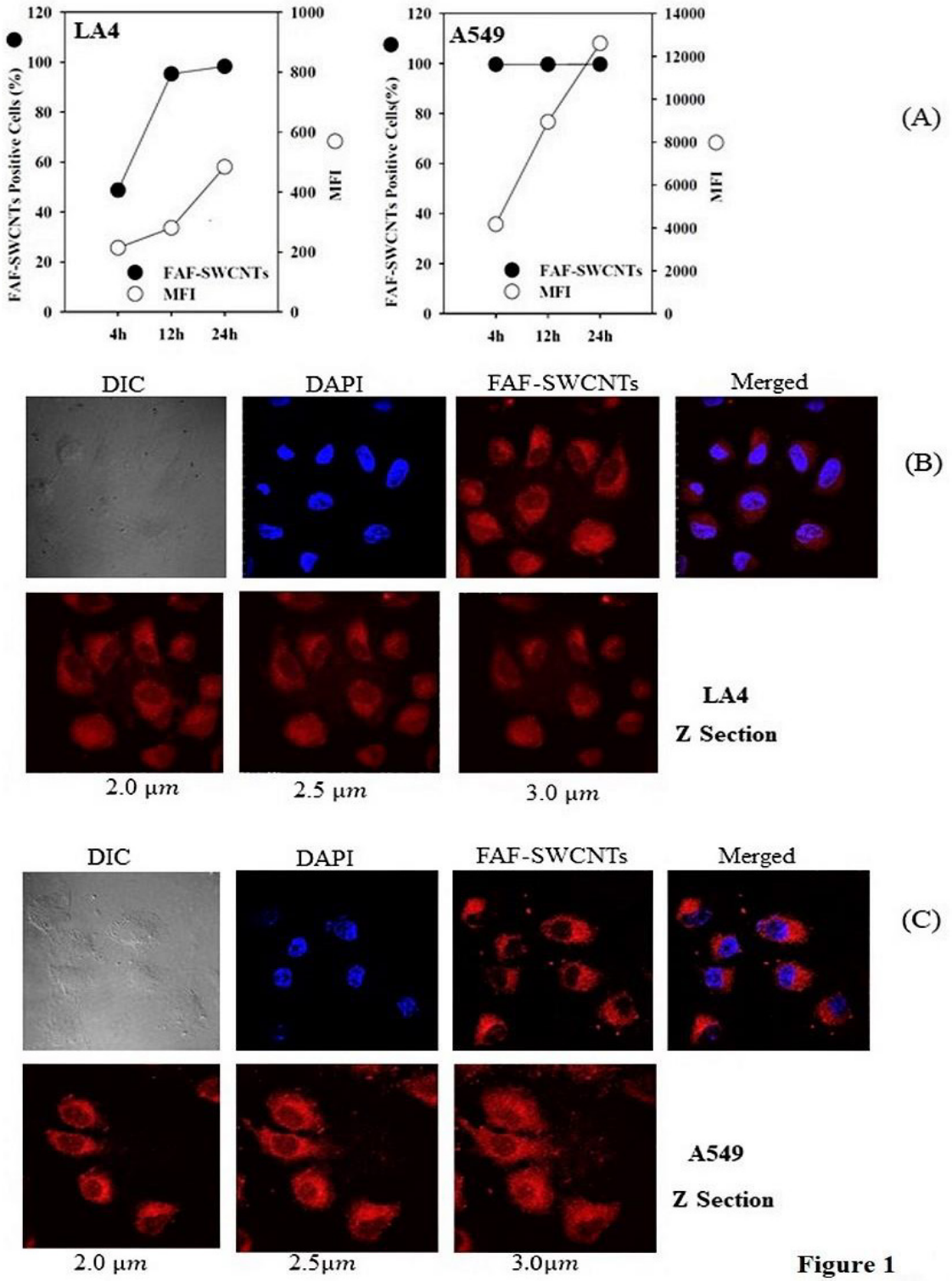

Figure 1

Figure 1: Uptake and Localization of Fluorescence-tagged-AF-SWCNTs (FAF-SWCNTs) by LA4 and A549 cells. LA4 and A549 Cells [0.2×106/ml/well] were cultured with FAF-SWCNTs (10 μg/ml) for up to 24 hours. After incubation, cells were washed with PBS, detached using trypsin, and analyzed on a flow cytometer to evaluate the uptake of FAF-SWCNTs by LA4 and A549 cells. Panel A shows the kinetics of uptake of FAF-SWCNTs by LA4 and A549 cells, where left Y-axis shows percentage of cells that were FAF-SWCNTs positive and right Y-axis shows mean fluorescence intensity (MFI) for the uptake of FAF-SWCNTs. Each plotted value is a Mean±SEM of 3 individual experiments. Confocal microscopy results are shown in panels B (LA4 cells) and C (A549 cells). In each panel B and C, upper set of micrographs show FAF-SWCNTs uptake (red fluorescence) and nuclei are defined by blue stain of Hoechst 33342 dye, and lower set shows z-sectioning at 2, 2.5 and 3 micron depths. Magnifications 100X in all cases. DIC stands for Differential Interference Contrast .

.

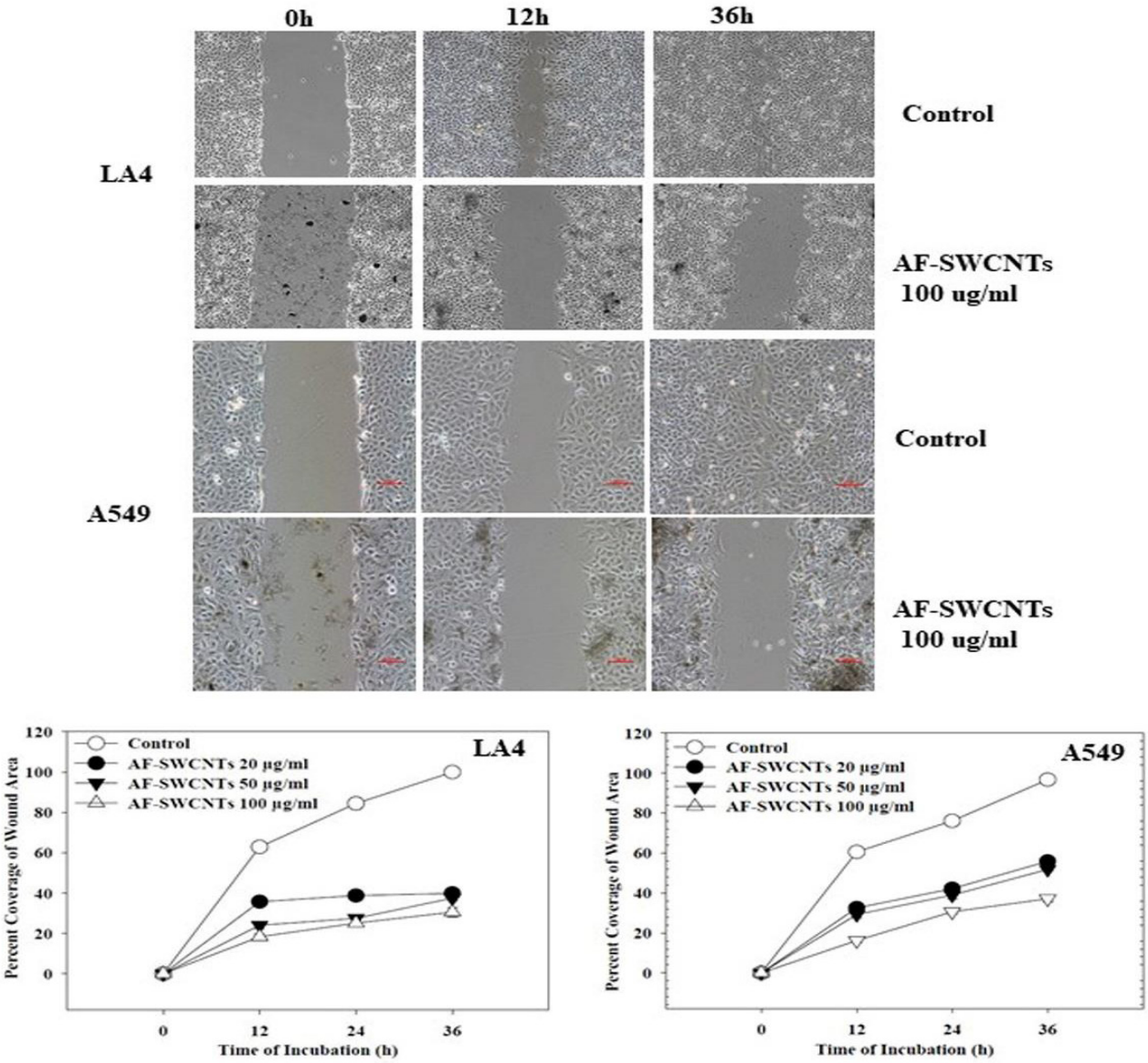

Figure 2: Effect of AF-SWCNTs on the in vitro wound repair process in LA4 and A549 cell monolayers. LA4 and A549 cells [0.5x10⁶/ml/well] were cultured in 12 well plate to get confluent monolayers, after which cells were incubated with or without AF-SWCNTs [20, 50 and 100 µg/ml] for 6 hours. Uniform scratches were made in the monolayers and the wounded monolayers were washed with fresh medium and media replaced with AF-SWCNTs suspensions at original concentrations. Photographs were taken at 0, 12, 24 and 36 hours post wounding using a Nikon phase contrast microscope. Top panel shows representative images of the wound repair process in control and AF-SWCNTs (100 µg/ml) exposed LA4 and A549 cells, at 0, 12 and 36 h time points. Area of the residual scratch wounds at 0, 12, 24 and 36 h time points were measured with Image-J software and the kinetics of the filling of scratch wound is shown in the lower panel. Each plotted value represents mean ± SEM of 9 random measurements in three individual experiments. SEM values were too small to be visible on the plot. At each concentration of AF-SWCNTs, the statistical significance of difference between the control and AF-SWCNT treatment curves was highly significant ($p<0.001$).

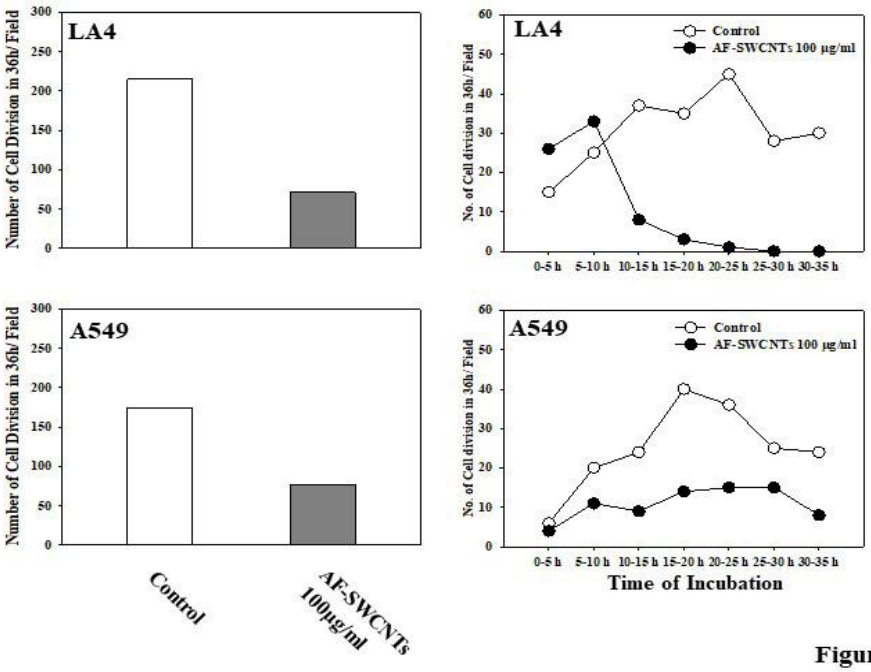

Figure 3

Figure 3: : Effect of AF-SWCNTs on cellular migration and proliferation during wound healing of scratched LA4 and A549 cell monolayers, observed by live imaging time-lapse photography. Wound repair process was examined by time lapse videography as described in methods. Actual numbers of cell divisions around the wounded area in LA4 and A549 monolayers over the time span of 36 hours could be counted from the video clips that can be viewed on flowing links: https://youtu.be/cM4oZ57zzzo (LA4 Control); https://youtu.be/uY94V1s1yS0 (LA4 with AF-SWCNTs); https://youtu.be/Nv7vCil1L8U (A549 Control); https://youtu.be/nx_lPWdN6kU (A549 with AF-SWCNTs). Left panels show the total number of cell divisions in the complete view fields in 36 hours for control and AF-SWCNTs treated cells. Right panels show the number of cell divisions during 5-hour intervals starting from 0 hours to 35 hours per field in control and AF-SWCNTs exposed LA4 and A549 cells.

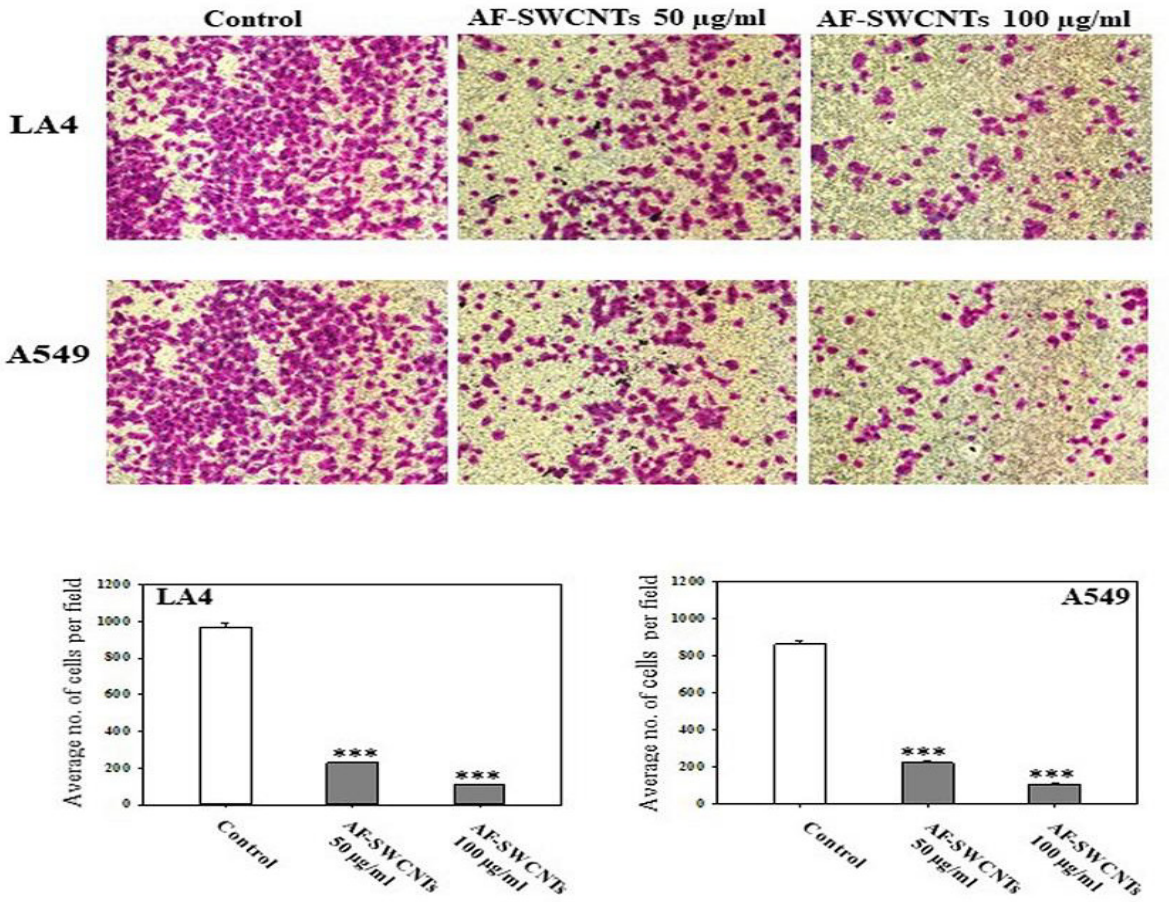

Figure 4: Effect of AF-SWCNTs on the cell migration of LA4 and A549 cells through a porous membrane using Transwell assay plates. Migration of cells across the permeable membrane was examines as described in methods. Top panel images show the migration of control cells and cells treated with 50 or 100 µg/ml of AF-SWCNTs. Bottom panel shows the quantitative evaluation of average number of cells migrated per field in control and AF-SWCNTs exposed LA4 and A549 cells. Each bar represent mean ± SEM of 9 random fields in three individual experiments. Inhibition of migration in AF-SWCNTs exposed cells was highly significant (***p<0.001).

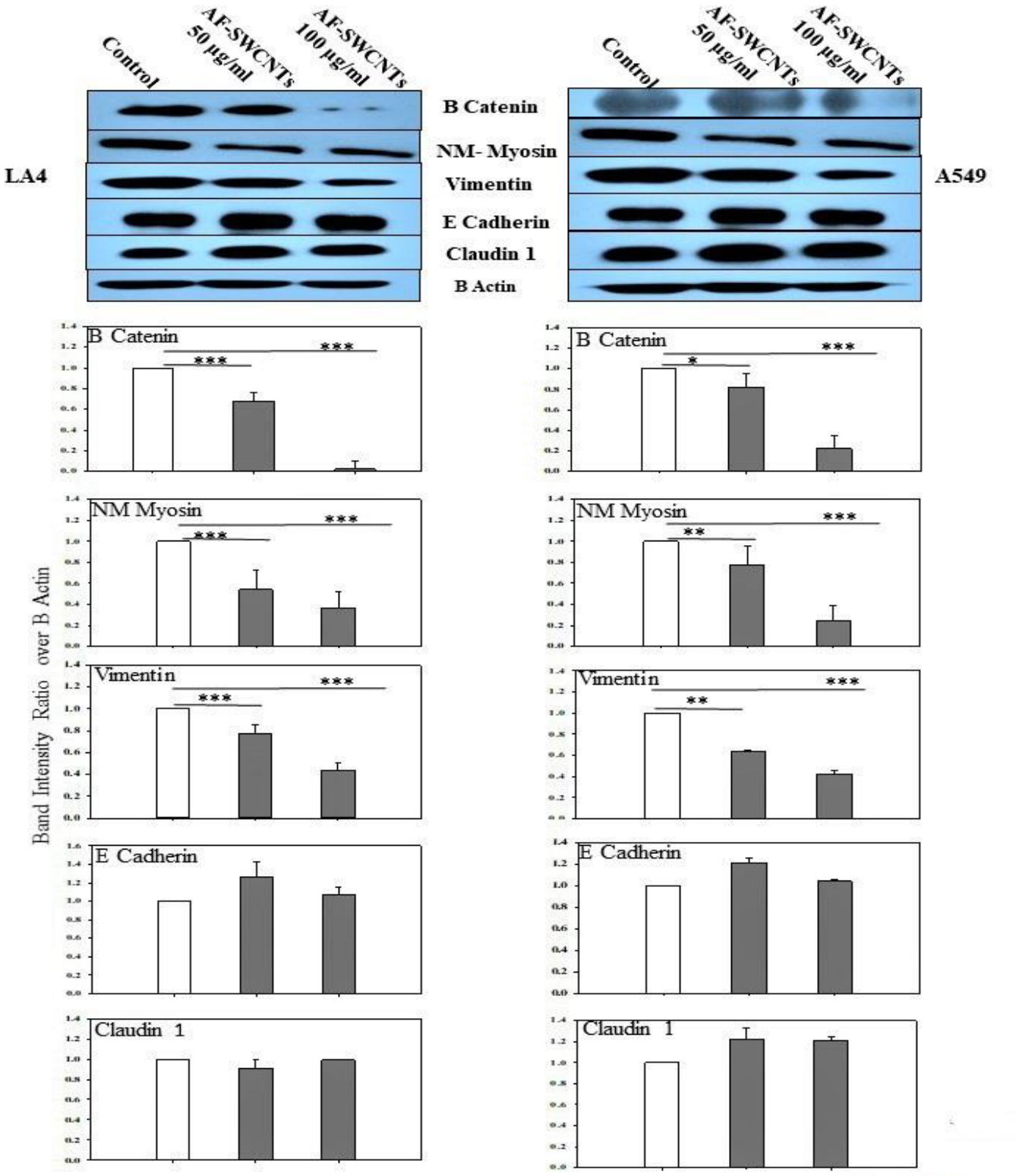

Figure 5: Expression of key protein markers involved in cellular adhesion and migration in control and AF-SWCNTs treated LA4 and A549 cells by western blotting.LA4 and A549 cells [0.5 × 106/ml/well] were seeded in wells of 6 well plate with or without AF-SWCNTs [50 or 100 µg/ml] for 48 hrs. Protein lysates were prepared and analyzed by Western blotting as described in methods. Histograms show result of 3 independent experiment (Mean ± SEM). Differences are significant from control with *p<0.05, **p<0.01, ***p<0.001.

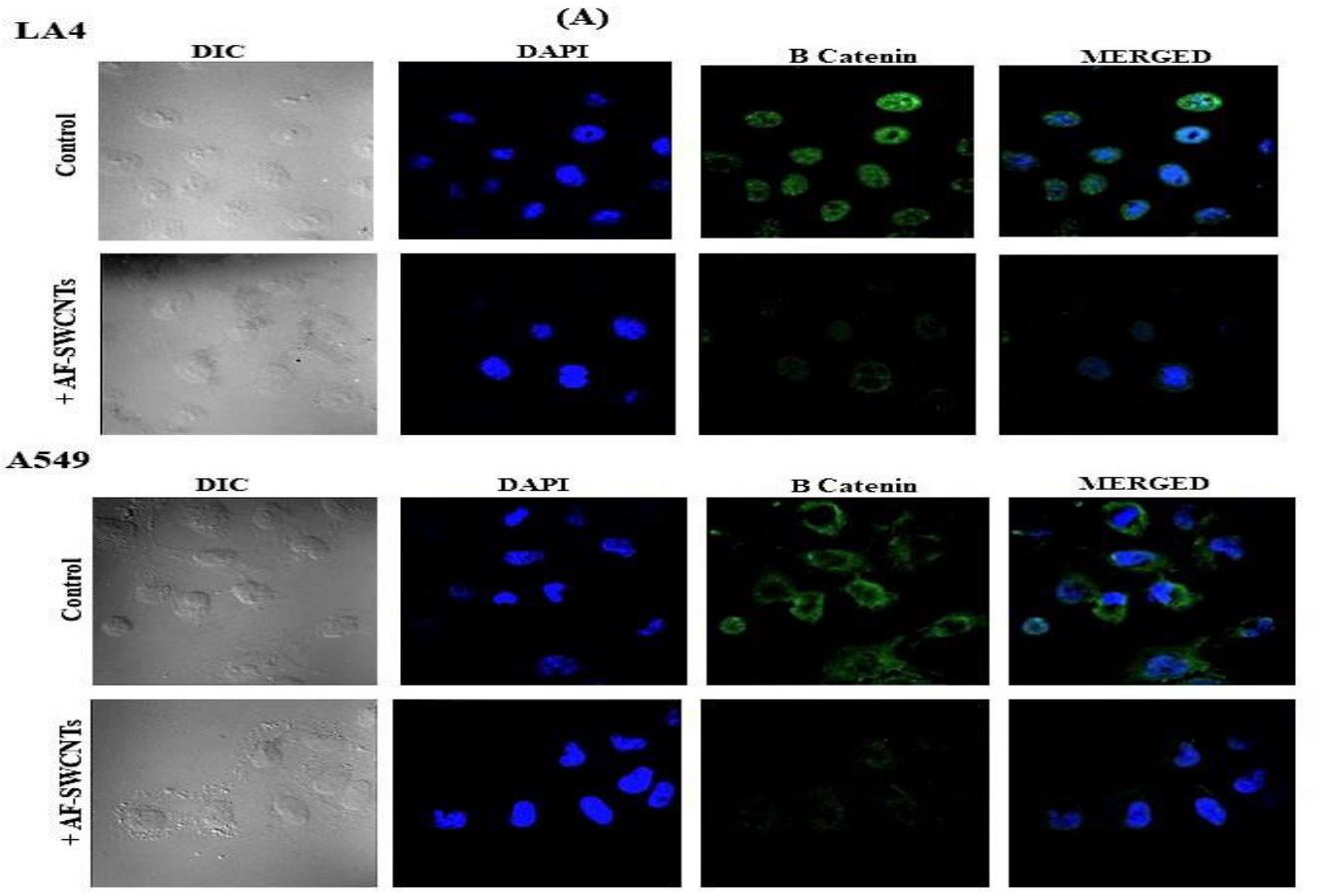

Figure 6 A

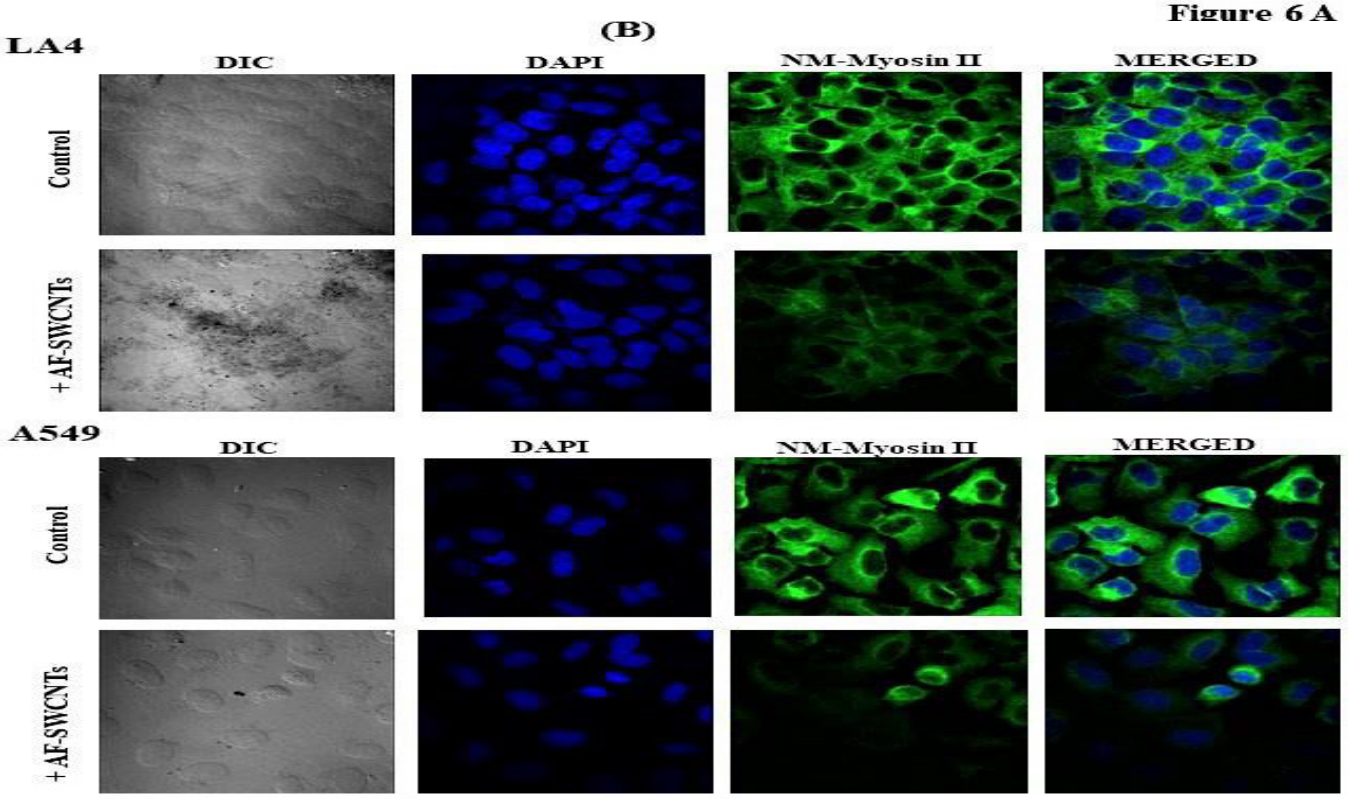

Figure 6 B

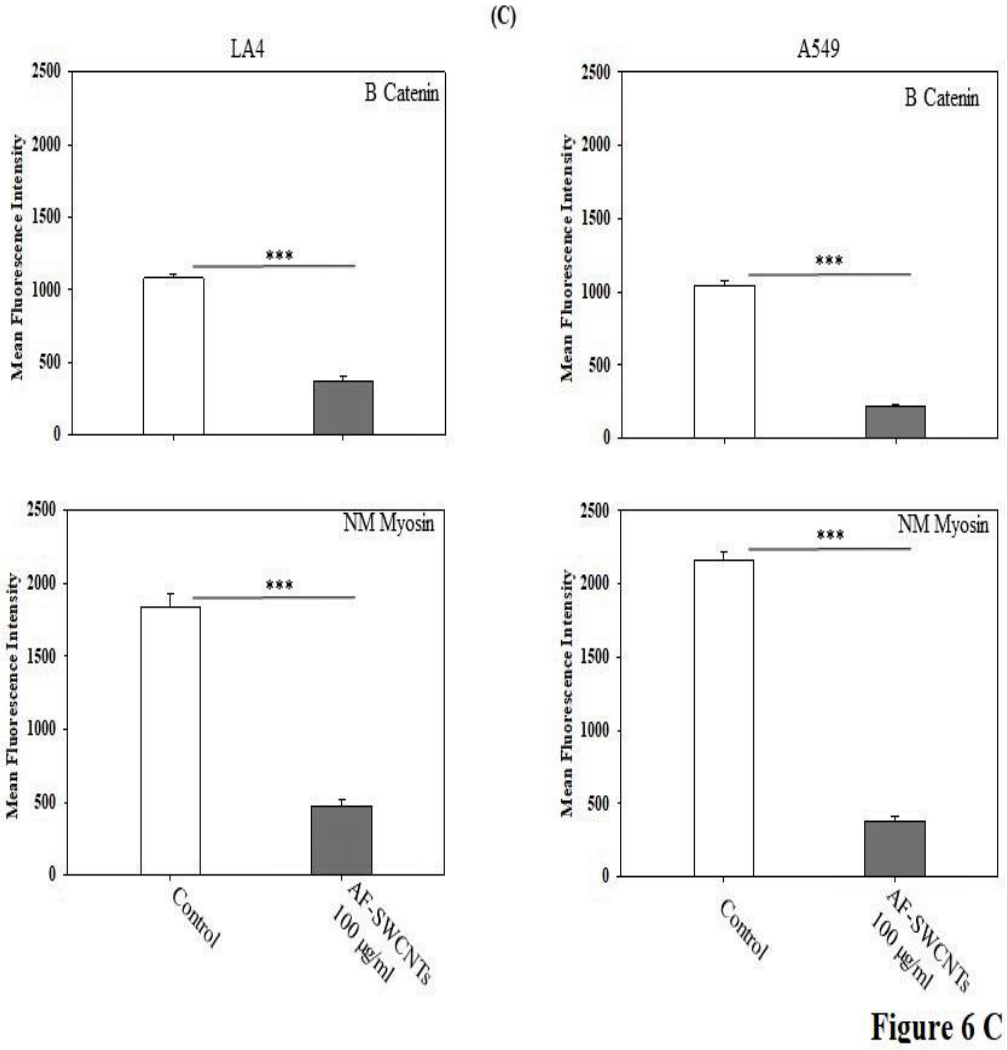

Figure 6: Effect of AF-SWCNTs on the expression of ß-catenin and NM-Myosin in LA4 and A549 cells by Immunofluorescence assay. Results in part A show the distribution of ß-catenin stain in LA4 cells with or without AF-SWCNTs (top two panels) and similar data for A549 cells (bottom two panels). Part B shows the same data for NM-myosin stain. Mean fluorescence intensity (MFI) was calculated from 8 different portion of slides in an automated manner that considers the intensity per cell in each portions of the slides. Part C shows quantitative differences in the MFI of control and AF-SWCNTs treated LA4 and A549 cells (mean ±SEM). Differences are significant from control with ***p<0.001.

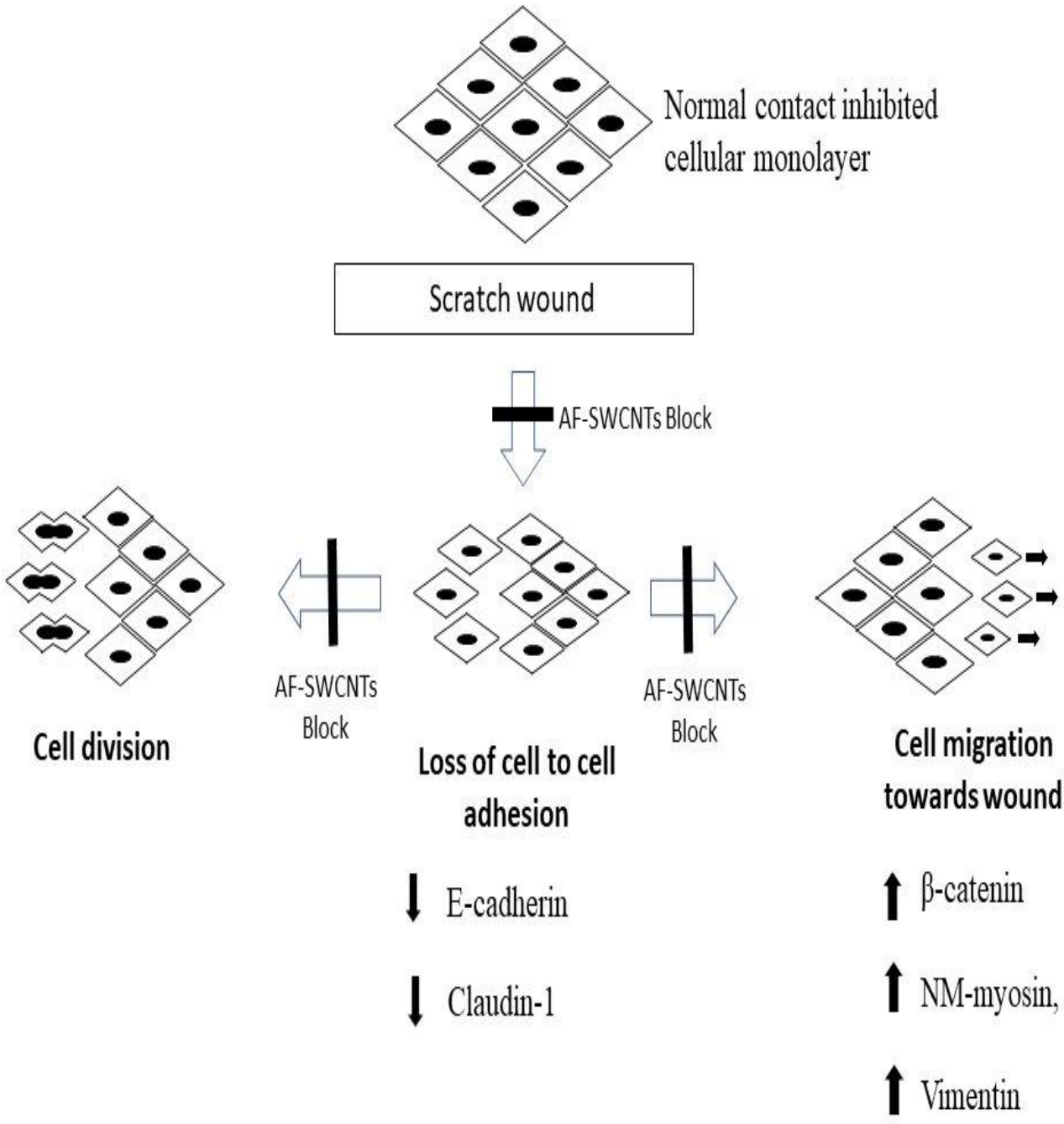

Figure 7: Summary model. A model depicting the changes in cellular functions that are required for the process of wound healing and their inhibition by the AF-SWCNTs.

Supplementary Figure 1

Characterization of AF-SWCNTs

Panel A shows the Zeta potential and Zeta size of AF-SWCNTs (Our data using Zeta Sizer). Panel B shows the TEM image of AF-SWCNTs (Our data). Panel C shows the mid- and near-infrared spectroscopic results (Data from Sigma-Aldrich).

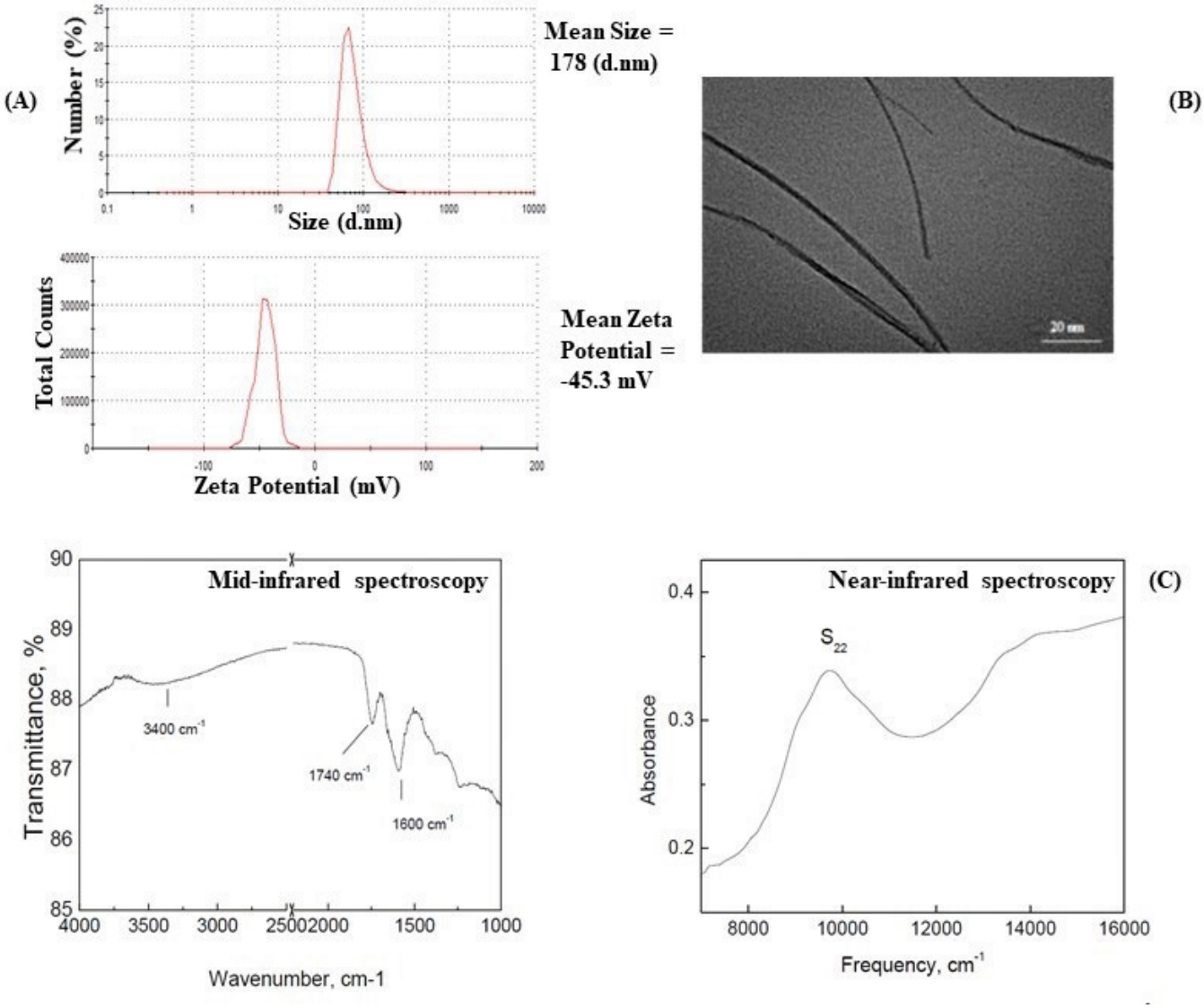

Expression of β-catenin and NM-myosin in control and AF-SWCNTs exposed cells was further examined by immunofluorescence microscopy. For this purpose, cells were cultured with or without 100 µg/ml of AF-SWCNTs for 24 hours, fixed, permeabilized and stained with various antibodies as described in methods. Results in Figure 6A and 6B show that AF-SWCNTs exposed cells showed decreased fluorescence intensity of both markers compared to control cells (Figure 6A for β-catenin expression, Figure 6B for NM-myosin expression). Quantitative analysis of mean fluorescence intensity plot (Figure 6C) indicates significantly lower fluorescence intensity values as compared to the control cells in case of both LA4 and A549 cells. These results confirmed the western blot results for these two markers.

Discussion

Two lung epithelial cell lines [a mouse (LA4) and a human (A549)], used in the present study have extensively been used as models for studying lung epithelial cells function [31, 32]. While both cell lines efficiently internalized AF-SWCNTs and showed 100% positivity for AF-SWCNTs after 12 hours of incubation. Confocal laser microscopy and Z-sectioning studies revealed that most of the internalized carbon nanotubes were localized in the cytoplasmic space while a much smaller number transgressed nuclear membrane and was visible inside the nucleus. The mechanism of uptake of carbon nanotubes is complex and many uptake mechanisms like receptor-mediated or non-receptor mediated endocytosis, diffusion, membrane fusion, or direct pore transport of the extracellular material into the cell may contribute to

this process [33, 34]. Several parameters such as the size, length, nature of functional groups, hydrophobicity and surface chemistry of CNTs play crucial roles in the process of internalization into cells [33, 34, 35-38]. The process seems to be partially energy dependent as the AF-SWCNTs uptake is lower at 4°C as compared to 37°C [15]. The piercing nature resulting from its needle-like structure may also be a determining factor for the nanotubes to enter into the cell through the cell membrane [15, 37-39]. AF-SWCNTs blocked the ability of both cells to repair scratch wounds (Figure 2). We used the live-cell imaging system to obtain time-lapse video clips of the two cells moving in to fill the void created by scratch. Time-lapse videography brings into focus two interesting features of wound healing in this system. Firstly, (a) significant cell division activity was observed around the area of scratch wound, and (b) migration of cells from the edge towards the scratch gap was clearly seen for both cells. Kinetics of change in cell proliferation activity recorded in the video clips (Video clip1) show that while in the case of control cells, cell division activity continued throughout, in AF-SWCNTs treated LA4 cells (Video clip2), the proliferative activity ceased all together after 15 hours. In A549 cells, proliferation continued albeit at a significantly lower rate. In LA4 cells, the filling of the scratch gap also stopped after 12 hours-time-point that correlated with the stoppage of cell division activity. Migration of cells was significantly suppressed in A549 cells also but interestingly, some filling of the wound area appeared to have continued after 12 hour time point as suggested by the slopes of the wound space filling kinetics curves between 12 h to 36 h time points (Figure 3 lower right panel). It is possible that continued cell division, even though at lesser rate, could be a factor in gap filling after 12 hours in A549 cells. In the scratch wound healing system, both cell division as well as cell migration could be factors in the filling of the scratch gap. In another system of cell migration across trans-well membrane, potent inhibitory effect of AF-SWCNTs could be seen on cellular migration. Cell division activity may not be a prominent factor determining migration in the trans-well assay and these results clearly indicate that cell migration of both cells was blocked by exposure to AF-SWCNTs. It can be conceived that in lung epithelial cell layer repair in vivo as well as in scratch wound repair assay in vitro, moving cells would have to get detached from surrounding cells of the monolayer and initiate the process of migration. It was therefore important to assess the expression levels of molecules that participate in cell adhesion and migration and determine the effect of AF-SWCNTs on the expression of these molecules. We selected five crucial proteins β-catenin, NM-myosin II, Vimentin, E-cadherin and Claudin-1, which play important roles and are associated with the cell migration process [40-42]. Significant decrease in the expression of β-catenin, NM-myosin II and Vimentin were observed in both LA4 and A549 cells exposed to AF-SWCNTs with respect to the control cells. β-catenin is the master regulator of the Wnt signaling pathway that drives the expression of genes necessary for the epithelial to mesenchymal transition associated with cell motility [42, 43]. For cell movement, the contraction force is provided by NM-myosin II protein at the leading edge that coordinates with actin polymerization and is essential for wound closure. The contractility of myosin also plays a strong role in directional migration and polarization of migration machinery [40, 41, 44]. Vimentin promotes cell migration process by guiding the growth of microtubule in epithelial cells. In addition to increasing cell motility, it also induces physical changes in cell shape, loss of cell-cell contacts, and increased turnover of focal adhesions, factors recognized as crucial for migration and metastasis of cancer cells also. Integration of mechanical input from the environment and the dynamics of microtubules and the actomyosin network play crucial roles in vimentin promoted cell migration process [45-47]. In AF-SWCNTs exposed LA4 and A549 cells, we found no significant changes in the expression of E-cadherin and Claudin -1 with respect to the control which was expected when cell migration is inhibited. E-cadherin is a key molecule of adherens junctions that serves as bridges connecting the cytoskeleton of neighboring cells through direct interaction. Numerous studies have suggested a tumor suppressor role of E-cadherin and Claudin-1 as downregulation of their expression occurs in invasive cancer cells [48-50]. E-cadherin and Claudin-1 are important components of the tight junctions responsible for cell–cell adhesion [50-52]. Immunofluorescence studies indicated a sharp decline in the expression of ß-catenin and NM-myosin-II in AF-SWCNTs exposed cells. This finding confirmed the results obtained by western blotting protein analysis.In summary, we have demonstrated that the three factors of cell division, adhesion and migration that play central role in wound healing process in vitro, are all modulated by AF-SWCNTs. A model depicting the summary of our findings is given in Figure 7.

Funding

This work was supported by Department of Science and Technology, Government of India, Nano-sciences Mission grant number SR/NM/NS-1219 and JC Bose award to RKS. SPB received fellowship support from the Indian Council of Medical Research, New Delhi.

Disclosure Statement

Authors report no conflicts of interest.

Acknowledgement

Research funding from the Department of Science and Technology, Government of India, and fellowship support to SPB from ICMR are gratefully acknowledged.

References:

1. Lijima, S (1991) Helical microtuble of graphitic carbon. Nature, 354, 56-58.
2. Chen, J. & Yan, L (2017) Recent Advances in Carbon Nanotube-Polymer Composites. Advances in Materials, 6(6): 129-148.
3. Rezaee M., Behnam B., Banach M. & Sahebkar A (2018) The Yin and Yang of carbon nanomaterials in atherosclerosis. Biotechnology Advances, 36(8): 2232-2247.
4. Yudasaka M., Yomogida Y., Zhang M., Nakahara M. & Koboyashi N., et al (2018) Fasting dependent vascular permeability enhancement in brow adipose tissues evidenced by using carbon nanotubes as fluorescent probes. Scientific Reports, 8(1): 14446.
5. Schroeder, V., Savagutrup, S., He, M., Lin, S. & Swager T.M (2019) Carbon nanotube chemical sensors. Chemical Reviews, 119 (1): 599–663.
6. Helland, A., Wick, P., Koehler, A., Schmid, K. & Som, C (2007) Reviewing the Environmental and Human Health Knowledge Base of Carbon Nanotubes. Environment Health Perspective, 115(8): 1125–31.
7. Poland, C.A., Duffin, R., Kinloch, I., Maynard, A., Wallace, W.A., Seaton, A., Stone, V., Brown, S., MacNee, W. & Donaldson, K (2008) Carbon nanotubes introduced into the abdominal cavity of mice show asbestos like pathogenicity in a pilot study. Nature Nanotechnology, 3(7): 423-28.
8. Sachar, S. & Saxena, R.K (2011) Cytotoxic effect of poly-dispersed single walled carbon nanotubes on erythrocytes in vitro and in vivo. PLoS One, 6(7): e22032.
9. Jackson, P., Jacobsen, N.R., Baun, A., Birkedal, R., Kühnel, D., Jensen, K.A., Vogel, U. & Wallin, H (2013) .Bioaccumulation and ecotoxicity of carbon nanotubes. Chemistry Central Journal, 7(1): 154.
10. Wang, Y., Iqbal, Z. & Mitra, S (2006) Rapidly functionalized, water dispersed, Carbon nanotubes at high concentration. Journal of American Chemical Society, 128(1): 95-99.
11. Saxena, R.K., Williams, W., Mcgee, J.K., Daniels, M.J., Boykin, E. & Ian Gilmour, M (2007) Enhanced in vitro and in vivo toxicity of poly-dispersed acid-functionalized single-wall carbon nanotubes. Nanotoxicology, 1, 291-300.
12. Gazia A. & El-Magd M.A (2019) Effect of pristine and functionalized multi walled carbon nanotubes on rat renal cortex. Acta Histochemical, 121(2): 207-217.
13. Alam, A., Sachar, S., Puri, N. & Saxena, R.K (2013) Interactions of poly-dispersed single-walled carbon nanotubes with T-cells resulting in downregulation of allogeneic CTL responses in vitro and in vivo. Nanotoxicology, 7(8): 1351–60.
14. Dutt, T.S. & Saxena, R.K (2019a) Activation of T and B lymphocytes Induces Increased Uptake of Poly-Dispersed single-Walled Carbon Nanotubes and Enhanced Cytotoxicity. International Journal of Nanotechnology in Medicine & Engineering, 4:3, 16-25.
15. Dutt, T.S., Mia B.M. & Saxena, R.K (2019) Elevated internalization and cytotoxicity of poly-dispersed single-walled carbon nanotubes in activated B cells can be basis for preferential depletion of activated B cells in vivo. Nanotoxicology, 13(6):849-60.
16. Kumari, M., Sachar, S. & Saxena, R.K (2012) Loss of proliferation and antigen presentation activity following internalization of polydispersed carbon nanotubes by primary lung epithelial cells. PloS One, 7(2): e31890.
17. Abbas, Z., Puri, N. & Saxena, R.K (2015) Lipid antigen presentation through CD1d pathway in mouse lung epithelial cells, macrophages and dendritic cells and its suppression by poly-dispersed single-walled carbon nanotubes. Toxicology in vitro, 29(6): 1275 – 82.
18. Dutt, T.S. & Saxena, R.K (2019b) Enhanced antibody response to ovalbumin coupled to poly-dispersed acid functionalized single walled carbon nanotubes. Immunology Letters, 217:77-83.
19. Bhardwaj N. & Saxena R.K (2015) Selective loss of younger erythrocytes from blood circulation and changes in erythropoietic patterns in bone marrow and spleen in mouse anemia induced by poly-dispersed single wall carbon nanotubes. Nanotoxicology, 9(8): 1032-40.
20. Crosby, LM. & Waters, CM (2010) Epithelial repair mechanisms in the lung. American Journal of Physiology. Lung Cellular Molecular Physiology, 298(6): L715-31.
21. Gardner, A., Borthwick, L.A. & Fisher, A.J (2010) Lung epithelial wound healing in health and disease. Expert Reviews of Respiratory Medicine, 4(5): 647–60.
22. Manicone, A.M (2009) Role of the pulmonary epithelium and inflammatory signals in acute lung injury. Expert Review of Clinical Immunology, 5(1): 63–75.
23. Ghosh, C.M., Makena, S.P., Kennedy, J., Teng, B., Luellen, C., Sinclair, S.E. & Waters C. M (2017) A heteromeric molecular complex regulates the migration of lung alveolar epithelial cells during wound healing. Scientific Report, 7(1): 2155.
24. Olajuyin, A.M., Zhang X. & Ji, H-L (2019) Alveolar type 2 progenitor cells for lung injury repair. Cell Death Discovery, 5, 63.
25. Singh, A. P., Mia M.B. & Saxena, R.K (2020) Acid-functionalized single walled carbon nanotubes alter epithelial tight junctions and enhance paracellular permeability. Journal of Biosciences, 45, 23.
26. Liang, CC., Park, AY. & Guan JL (2007) In vitro scratch assay: a convenient and inexpensive method for analysis of cell migration in vitro. Nature Protocols, 2(2): 329–33.
27. Cory, G (2011) Scratch-wound assay. Methods in Molecular Biology, 769: 25-30.
28. Chen, Y (2012) Scratch wound healing assay. Bio protocols, 2(5): e100.
29. Lohcharoenkal, W., Wang, L., Stueckle A.T., Dinu Z.C., Castranova, V., Liu, Y. & Rojanasakul, Y (2013) Chronic Exposure to Carbon Nanotubes Induces Invasion of Human Mesothelial Cells through Matrix Metalloproteinase-2. American Chemical Society Nano, 7(9): 7711-23.
30. Chen, X., Wang, H., Li, D., Yu, Y. & Zhi, J (2016) The effect of carboxylated nanodiamond (cNDs) on the migration of HepG2 cells. Physica Status Solidi, 213, 2131-37.
31. Sonar SS., Schwinge, D., Kilic, A., Yildirim, A.Ö., Conrad, M.L., Seidler, K., Müller, B., Renz, H. & Nockher, W.A (2010) Nerve growth factor enhances Clara cell proliferation after lung injury. European Respiratory Journal, 36, 105-15.
32. Ren, H., Birch, N.P. & Suresh, V (2016) An Optimised Human Cell Culture Model for Alveolar Epithelial Transport. PLoS One, 11(10): e0165225.
33. Lee, Y. & Geckeler, K. E (2010) Carbon nanotubes in the biological interphase: the relevance of non covalence. Advanced Materials, 22(36): 4076–83.
34. Rastogi, V., Yadav, P., Sankar S., Bhattacharya, SS., Mishra, AK., Verma N. & Pandit JK (2014) Carbon Nanotubes: An Emerging Drug Carrier for Targeting Cancer Cells. Journal of Drug Delivery. Journal of Drug Delivery, Article ID 670815.
35. Oberdörster, G (1996) Significance of particle parameters in the evaluation of exposure-dose-response relationships of inhaled particles. Particulate Science and Technology, 14(2),135-51.
36. Veronesi, B., Haar de C., Lee L. & Oortgieson, M (2002) The Surface Charge of Visible Particulate Matter Predicts Biological Activation in Human Bronchial Epithelial Cells. Toxicology and Applied Pharmacology, 178(3): 144–54.
37. Nagai, H. & Toyokuni S (2012) Differences and similarities

between carbon nanotubes and asbestos fibres during mesothelial carcinogenesis: shedding light on fiber entry mechanism. Cancer Science, 103(8): 1378-90.
38. Lacerda, L., Russier J., Pastorin, G., Herrero MA., Venturelli, E., Dumortier, H., Al-Jamal, KT., Prato, M., Kostarelos, K. & Bianco, A (2012) Translocation mechanisms of chemically functionalised carbon nanotubes across plasma membrane. Biomaterials, 33(11): 3334-43.
39. Shvedova, A.A., Pietroiusti, P., Fadeel, B. & Kagan, V.E (2012) Mechanisms of carbon nanotube induced toxicity: Focus on oxidative stress. Toxicology and Applied Pharmacology, 261(2): 121-33.
40. V-Manzanares, M., Ma, X., Adelstein, RS. & Horwitz, AR (2009) Non-muscle myosin II takes centre stage in cell adhesion and migration. Nature Reviews. Molecular Cell Biology, 10(11): 778-90.
41. Devreotes, P. & Horwitz, A.R (2015) Signaling Networks that Regulate Cell Migration. Cold Spring Harbour Perspective of Biology, 7(8): a005959.
42. Yang, C.M., Ji S., Li Y., Fu L.Y., Jiang T. & Meng, F.D (2017) ß-catenin promotes cell proliferation, migration, and invasion but induces apoptosis in renal cell carcinoma. Oncotargets and Therapy, 10, 711–24.
43. Muller, T., Bain, G., Wang, X. & Papckoff, J (2002) Regulation of Epithelial Cell Migration and Tumour Formation by β-Catenin Signaling. Experimental Cell Research, 280(1): 119-33.
44. Tamada, M., Perez, D.T., Nelson J.W. & Sheetz P.M (2007) Two distinct modes of myosin assembly and dynamics during epithelial wound closure. The Journal of Cell Biology, 176(1): 27–33.
45. Mendez, MG., Kojima, S. & Goldman, RD (2010) Vimentin induces changes in cell shape, motility, and adhesion during the epithelial to mesenchymal transition. Federation of American Societies of Experimental Biology, 24(6):1838–51.
46. Rogel, MR., Soni, PN., Troken, JR., Sitikov, A., Trejo, HE. & Ridge, KM (2011) Vimentin is sufficient and required for wound repair and remodelling in alveolar epithelial cells. Federation of American Societies of Experimental Biology, 25(11): 3873–83.
47. Battaglia, R.A (2018) Vimentin on the move: new development on the cell migration. F1000 Research. 7. PMID: 30505430.
48. Gottardi, C.J., Wong, E. & Gumbiner, BM (2001) E-Cadherin suppresses cellular transformation by inhibiting β-Catenin signalling in an adhesion-independent manner. Journal of Cell Biology, 153 (5): 1049-60.
49. Pećina-Slaus, N (2003) Tumor suppressor gene E-cadherin and its role in normal and malignant cells. Cancer Cell International, 3(1):17.
50. Zhou, B., Moodie, A., Blanchard, A.A., Leygue, E. & Myal, Y (2015) Claudin 1 in Breast Cancer: New Insights. Journal of Clinical Medicine, 4(12):1960-76.
51. Frixen, UH., Behrens, J., Sachs, M., Eberle, G., Voss, B., Warda, A., Löchner, D. & Birchmeier, W (1991) E-cadherin-mediated cell-cell adhesion prevents invasiveness of human carcinoma cells. Journal of Cell Biology, 113(1), 173–85.
52. Zhai, B., Yan, H.X., Liu, S.Q., Chen, L., Wu, M.C. & Wang, H.Y (2008) Reduced expression of E-cadherin/catenin complex in hepatocellular carcinomas. World Journal of Gastroenterology, 14(37): 5665–73.